

Optimized Schwarz waveform relaxation for nonlinear systems of parabolic type

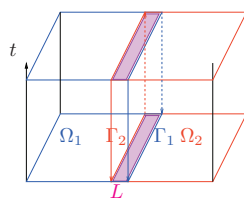
Florian Häberlein¹ and Laurence Halpern¹

1 Schwarz waveform relaxation algorithms for a linear system

Let \mathcal{L} be a partial differential operator, possibly acting on vector functions $(x, t) \mapsto u(x, t) \in \mathbb{R}^d$, of the time variable t and the space variable $x = (x_1, x_2)$. The equation to be solved in $\Omega \times (0, T)$ is

$$\mathcal{L}u = F \text{ in } \Omega \times (0, T), \quad u(\cdot, 0) = u_0 \text{ in } \Omega, \quad \mathcal{B}u = g \text{ on } \partial\Omega. \quad (1)$$

The domain Ω is split into subdomains Ω_i with possible overlap. Table 1 on the left shows the simplified case of a rectangle $\Omega = (A, B) \times (E, F)$ divided into two rectangles $\Omega_1 = (A, C+L) \times (E, F)$ and $\Omega_2 = (C, B) \times (E, F)$ with overlap L , this example will be the model case in the paper. On the right is described the alternate algorithm, via two *transmission operators* \mathcal{B}_j on Γ_j . Boundary conditions are enforced on the other boundaries, of Dirichlet or Nemann type. A parallel Schwarz algorithm for elliptic equations was introduced by P.L. Lions in [14], extending the original Schwarz's domain decomposition algorithm for the Laplace equation in [16].



$$\begin{cases} \mathcal{L}u_1^k = F \text{ in } \Omega_1 \times (0, T) \\ u_1^k(\cdot, 0) = u_0 \text{ in } \Omega_1, \mathcal{B}u_1^k = g \text{ on } \partial\Omega_1 \setminus \Gamma_1 \\ \mathcal{B}_1 u_1^k = \mathcal{B}_1 u_2^{k-1} \text{ on } \Gamma_1 \times (0, T) \end{cases}$$

$$\begin{cases} \mathcal{L}u_2^k = F \text{ in } \Omega_2 \times (0, T) \\ u_2^k(\cdot, 0) = u_0 \text{ in } \Omega_2, \mathcal{B}u_2^k = g \text{ on } \partial\Omega_2 \setminus \Gamma_2 \\ \mathcal{B}_2 u_2^k = \mathcal{B}_2 u_1^{k-1} \text{ on } \Gamma_2 \times (0, T) \end{cases}$$

Table 1: Domain decomposition and Schwarz waveform relaxation algorithm

P.L. Lions also mentioned the possibility of using the algorithm for time dependent problem. However, it was recognized and analyzed as a waveform algorithm (see [13]) only in [7]. The authors defined the *Schwarz waveform relaxation algorithm*, which uses as transmission operators $\mathcal{B}_j \equiv Id$, corresponding to *Dirichlet* transmission conditions. The convergence was analyzed with various tools, such as maximum principle, Laplace transform in time. This algorithm enjoys superlinear convergence over small time intervals, linear convergence over large time intervals. A more detailed historical account can be found in [10]. On large time intervals, a Fourier analysis is useful. Considering a small overlap, the boundaries of the do-

¹ LAGA, Université Paris 13, 99 Avenue J-B Clément, 93430 Villetaneuse, France, e-mail: halpern@math.univ-paris13.fr

mains can be rejected to infinity, and Fourier transform in the second variable can be performed. This is the simplest way to proceed, but Fourier series on bounded intervals can be used as well, though the objects are heavier, see [4] for an example in structure mechanics. Numerical results show that the parameters obtained through the analysis in an infinite domain are relevant.

Consider for instance the advection-diffusion reaction problem, with

$$\mathcal{L}u := \partial_t u + \mathbf{a} \cdot \nabla u - \nu \Delta u. \quad (2)$$

The algorithm for the error e_j^k is the same, with vanishing data F and u_0 . By Fourier transform in time and x_2 , with dual variables τ and ξ , the Fourier transforms are explicitly given by

$$\hat{e}_1^k(x_1, \xi, \tau) = \eta_1^k(\xi, \tau) e^{\frac{L-\tau}{2\nu}(a-f(z))}, \quad \hat{e}_2^k(x_1, \xi, \tau) = \eta_2^k(\xi, \tau) e^{\frac{\tau}{2\nu}(a+f(z))},$$

with notations which will remain throughout the paper

$$z(\xi, \tau) = i(\tau + a_2 \xi) + \nu \xi^2, \quad f(z) = \sqrt{a_1^2 + 4\nu z}.$$

The coefficients η_j^k are obtained recursively, using the transmission relations. They are governed by the convergence factor ρ_D , and given in the parallel case by

$$\rho_D(z, L) := e^{-\frac{L}{2\nu}f(z)}, \quad \eta_j^k = \rho_D(z, L)^k \eta_j^0.$$

ρ_D is identically equal to 1 when $L = 0$, so the algorithm is not convergent. For positive overlap, the high frequencies are damped exponentially. More precisely, for the rectangle case in Table 1, suppose the initial boundary value problem is solved by finite differences in time and space on a regular grid, with meshes Δt and $h = \Delta x_1 = \Delta x_2$. Suppose Dirichlet boundary conditions are enforced on $\partial\Omega$. Then the lowest frequency resolved by the grid on Γ_j is $\xi_m = \frac{\pi}{F-E}$, corresponding to a mode $\sin(\frac{\pi x_2}{F-E})$, while the highest frequency is $\xi_M = \frac{\pi}{h}$, corresponding to a mode $\sin(\frac{\pi x_2}{h})$. The highest and lowest frequencies in time are defined in the same way, by $\tau_m = \frac{\pi}{2T}$, $\tau_M = \frac{\pi}{\Delta t}$.

$$\tau_m = \frac{\pi}{2T}, \tau_M = \frac{\pi}{\Delta t}, \quad \xi_m = \frac{\pi}{F-E}, \xi_M = \frac{\pi}{h}, \quad K = z([\tau_m, \tau_M] \times [\xi_m, \xi_M]).$$

In this paper, we consider only implicit schemes, with Δt and h are comparable. Then the uniform convergence factor is given by

$$\sup_K |\rho_D(z, L)| \sim 1 - \frac{L}{2\nu} \operatorname{Re} f(\xi_m, \tau_m).$$

It tends linearly to 1 when the overlap tends to 0. For reasons of cost and memory, the overlap is usually a few mesh points only, which implies that the convergence

factor is highly dependent of the mesh size. It is therefore useful to design algorithms with a more robust convergence behavior.

Schwarz algorithms with Robin transmission conditions were proposed in [15], together with nonoverlapping subdomains. *Optimized Schwarz waveform relaxation algorithms* have afterwards been proposed, with or without overlap, to be able to accelerate the convergence of the algorithm. They use approximations of the Dirichlet-to-Neumann operator, they are differential in time and in the boundary variable, and take here the form

$$\mathcal{B}_{ju} := (\mathbf{n}_j)_1 (v \partial_1 u - \frac{a_1}{2} u) + \frac{p}{2} u + \frac{q}{2} (\partial_t u + a_2 \partial_2 u - v \partial_{22} u). \quad (3)$$

When $q = 0$, the operators are called *Robin* operators, while for $q \neq 0$, they are referred to as *Ventcel* operators. The coefficients p and q are calculated such that they optimize the convergence factor of the algorithm in the Fourier variables. Define a first degree polynomial $s(z) = p + qz \in \mathbf{P}_1$. The choice of p and q is a particular case of the best approximation problem in the space \mathbf{P}_n of complex polynomials with degree lower than n :

$$\rho(z, s, L) = \frac{s(z) - f(z)}{s(z) + f(z)} e^{-\frac{L}{2v} f(z)}, \quad |\rho(z^*, s^*, L)| = \inf_{s \in \mathbf{P}_n} \sup_{z \in K} |\rho(z, s, L)| := \delta_n^*(L). \quad (4)$$

The analysis of the best approximation problem for the advection-diffusion equation in one dimension in the Robin case ($n = 0$) has been made “by hand” in [6] for $\tau_m = 0$. Further general tools for well-posedness of the best approximation problem (4) have been set in [2] for the Robin case, and applied to the one-dimensional Ventcel-Schwarz algorithm. They are being extended in [1] to the 2-D case with a complete analysis and explicit asymptotic formulae. Well-posedness of the algorithm and convergence results, including variable coefficients and non planar boundaries in the nonoverlapping case, can be found in [11].

2 Optimized coefficients for the linear reactive transport system

We introduce a simplified system which has been used as a model in F. Häeberlein’s thesis on CO_2 sequestration. For the linearized system, we present optimized coefficients in closed form, extending previous results in [1]. A proof is given in the one-dimensional overlapping case, which is new. These coefficients will be used in the nonlinear case in §3.

Consider the system of equations for $\mathbf{u} = (u, v)$ in $\Omega \times (0, T)$,

$$\partial_t(\phi u) + \nabla \cdot (-v \nabla u + \mathbf{a}u) - R(u, v) = 0, \quad \partial_t(\phi v) + R(u, v) = 0, \quad (5)$$

where Ω is a bounded domain in \mathbb{R}^d and u and v denote the concentration of the mobile and fixed species, respectively. $\phi > 0$ is the porosity which is supposed to be constant in time, $v \geq 0$ is the scalar diffusion-dispersion coefficient, $\mathbf{a} \in \mathbb{R}^d$ is

the Darcy velocity. All physical properties are supposed to be given and constant in time. $R(u, v)$ is a nonlinear function representing the chemical coupling term. The final goal is to be able to simulate general situations where the kinetic reaction rate is fully nonlinear. We present in §3 a test case with a semilinear model $R(u, v) = k(v - \Psi(u))$, where $k > 0$ represents the reactive surface and Ψ is a nonlinear function modeling an adsorption process, see Figure 3, left. The domain decomposition process relies on obtaining good transmission conditions. Therefore we consider here a linear coupling term $R(u, v) = k(v - cu)$ where $k > 0$ represents the reactive surface and $c > 0$ an equilibrium constant. The linear case models a chemical reaction that reaches its equilibrium point at $v = cu$. By the same method of approximating the Dirichlet to Neumann map, Ventcell transmission conditions can be obtained:

$$\mathcal{B}_j \cdot \mathbf{u} := \pm(v\partial_1 - \frac{a_1}{2})u + \frac{p}{2}u + \frac{q}{2}(\phi\partial_t + a_2\partial_2 - v\partial_{22} + kc)u - \frac{q}{2}kv. \quad (6)$$

The convergence factor is still defined by (4), with z replaced by

$$Z(\xi, \tau, c) = z(\xi, \phi\tau) + kc \frac{i\phi\tau}{i\phi\tau + k}. \quad (7)$$

$Z(\xi, \tau, c)$ appears as a perturbation of the function $z(\xi, \phi\tau)$ introduced previously, and will be treated as a linear perturbation in the parameter c . The domain of optimization is $K(c) = Z([\tau_m, \tau_M] \times [\xi_m, \xi_M], c)$.

Warning: in this text, the proofs are based very often on asymptotic considerations. To alleviate the notations, we introduce the notation $Q \simeq h$ or $Q = \alpha(h)$ if there exists $C \neq 0$ such that $Q \sim Ch$. The analysis below is an extension of that made in the case $c = 0$ described above. The formulas include the case $c = 0$. The important theoretical results in [2, ?] apply here, to give

1. Existence of solutions for the best approximation problem, overlap or not.
2. Uniqueness for small $L, \Delta t$ and h , in the Robin case $n = 0$.
3. Uniqueness for $L = 0$, small Δt and h , in the Ventcel case $n = 1$.
4. For $n = 0$ and 1, consider the real function

$$F(s, L) = \sup_{Z \in K(c) \cap \{\Re Z \geq 0\}} |\rho(Z, s(Z), L)|. \quad (8)$$

If it has a local minimum in \mathbf{P}_n , it is the global minimum.

The last property will be decisive for the approximate computation of the best parameters.

Shortcuts are defined in one dimension by $f_m = f(Z(0, \tau_m, c))$, $f_M = f(Z(0, \tau_M, c))$.

Theorem 1. *For positive c , small $h \simeq \Delta t$, if $L = 0$ or $L \simeq h$, the best approximation problem (4) in $K(c)$ has a unique solution, whose coefficients are given in the 1-D case asymptotically in terms of $x_m = \Re(f(\tau_m))$, $x_M = \Re(f(\tau_M)) \sim \sqrt{\frac{2v\pi\phi}{\Delta t}}$.*

dimension	method	overlap	parameters (p^*, q^*)	$\delta^* \sim 1 - 2\frac{x_w}{p^*}$
1	$n=0$, Robin	$L=0$	$p_0^*(0) = \sqrt{\frac{x_m f_M ^2 - x_M f_m ^2}{x_M - x_m}}$	$1 - \alpha(\Delta t^{\frac{1}{4}})$
1	$n=0$, Robin	$L > 0$	$p_0^*(L) \sim p_0^*(0)$	$1 - \alpha(\Delta t^{\frac{1}{4}})$
1	$n=1$, Ventcel	$L \geq 0$	$p_1(L)^* \sim x_m^{\frac{3}{4}} x_M^{\frac{1}{4}}, \quad q_1^*(L) \sim \frac{2vp^*}{x_m x_M}$	$1 - \alpha(\Delta t^{\frac{1}{8}})$

In two dimensions, define, for $|a_2|\xi_m > \tau_m$, τ_0 as the largest real root of

$$\phi \tau \left(1 + c \frac{k^2}{k^2 + \tau^2 \phi^2} \right) = |a_2| \xi_m,$$

$$\text{the real function } g_1(s) = \frac{k^2}{s + k^2},$$

$$\xi_1 = a_2 \frac{(|\mathbf{a}|^2 + 4vkc(1 - g_1(\phi \tau_m))) - \sqrt{(|\mathbf{a}|^2 + 4vkc(1 - g_1(\phi \tau_m)))^2 + 16v^2(\phi \tau_m)^2(1 + cg_1(\phi \tau_m))^2}}{8v^2 \phi \tau_m (1 + cg_1(\phi \tau_m))},$$

$$Z_w = \begin{cases} Z(\xi_1, \tau_m) & \text{if } \xi_m \leq |\xi_1| \leq \xi_M, \\ Z(\tau_0, -\text{sign}(a_2)\xi_m) & \text{if } |\xi_1| \leq \xi_m \text{ and } \Re f(\tau_0, -\text{sign}(a_2)\xi_m) \leq \Re f(\tau_m, -\text{sign}(a_2)\xi_m), \\ Z(\tau_m, -\text{sign}(a_2)\xi_m) & \text{otherwise.} \end{cases}$$

$$x_w = \Re Z_w.$$

The best coefficients for the Robin-Schwarz algorithm ($n=0$) are

overlap	parameter p^*	$\delta^* \sim 1 - 2\frac{x_w}{p^*}$
$L=0$	$p_0^*(0) \sim \sqrt{\frac{2v\pi x_w \phi}{\Delta t}}$	$1 - \alpha(\Delta t^{\frac{1}{2}})$
$L > 0$	$p_0^*(L) \sim \sqrt[3]{\frac{v x_w^2}{2L}}$	$1 - \alpha(L^{\frac{1}{3}})$

Define the function

$$g(t) = \frac{2t - \sqrt{t^2 + 1}}{t^2 + 1},$$

and for $Q < Q_0 \approx 0.36900$, $t_2(Q)$ is the only root of $g(t) = Q$ larger than $t_0 = \sqrt{54 + 6\sqrt{33}}/6 \approx 1.567618292$,

$$P(Q) = \begin{cases} \sqrt{1 + \sqrt{t_2(Q)^2 + 1}} \left(\frac{1}{\sqrt{t_2(Q)^2 + 1}} + Q \right) & \text{if } Q < Q_1 \approx 0.1735, \\ 1 + Q & \text{if } Q > Q_1. \end{cases} \quad (9)$$

Defining $C = \Delta t/h$, the best coefficients for the Ventcel-Schwarz algorithm ($n=1$) are

overlap	p_1^*	q_1^*	$\delta^* \sim 1 - 2\frac{x_w}{p_1^*}$
$L=0$	$p_1^*(0) \sim \begin{cases} \sqrt[4]{\frac{v x_w^3 \pi}{h}} & \text{if } Cx_w < 2, \\ \sqrt[4]{\frac{8v x_w \pi}{hC(P(\frac{2}{Cx_w}))^2}} & \text{if } Cx_w > 2, \end{cases}$	$q_1^*(0) \sim \frac{2p_1^*(0)\pi}{hx_w}$	$1 - \alpha(h^{\frac{1}{4}})$
$L > 0$	$p_1^*(L) \sim \sqrt[5]{\frac{v x_w^4}{2L}}$	$q_1^*(L) \sim \frac{2v x_w^2}{p_1^*(L)^3}$	$1 - \alpha(L^{\frac{1}{5}})$

Proof. It relies on the use of the explicit formulations in [1] for $c = 0$, together with a continuation argument. We present in detail the analysis for the Robin transmission condition with overlap. Define

$$R_0(\tau, s) = \left| \frac{s - f(Z)}{s + f(Z)} \right|^2, \quad R(\tau, s, L) = R_0(\tau, s) e^{-L \Re f(Z)/v}. \quad (10)$$

Lemma 1. *In one dimension, for $\tau_M \gg 1$ and $L \ll 1$ with $L \asymp \tau_M^{-\lambda}$, the minmax problem (4) in $K(c)$ with $n = 0$ has a unique solution $(s_0^*(L), \delta_0^*(L))$.*

- If $0 < \lambda < \frac{3}{4}$, it is the unique solution of the equation

$$R(\tau_m, s, L) = R(\tau_+, s, L), \quad (11)$$

where $\tau_+(s, L)$ is the unique local maximum point of $R(\cdot, s, L)$. It is asymptotically given by

$$s_0^*(L) \sim \sqrt[3]{\frac{(\Re(f(\tau_m)))^2 L}{2v}} \quad \delta_0^*(L) \sim 1 - 2 \sqrt[3]{\frac{\Re(f(\tau_m)) L}{2v}}, \quad (12)$$

- If $\frac{3}{4} < \lambda \leq 1$, it is the unique solution of the equation

$$R(\tau_m, s, L) = R(\tau_M, s, L). \quad (13)$$

It is asymptotically given by

$$s_0^*(L) \sim s_0^*, \quad \delta_0^*(L) \sim \delta_0^*. \quad (14)$$

Remark 1. Note that if λ is close to 0, then $\delta_0^*(L) = 1 - \alpha \sqrt[3]{L}$, which gives the best behavior, independent of Δt . For the Dirichlet case, we would have

$$\sup_K |\rho_D(\tau, L)| = 1 - \alpha(L).$$

If $\lambda = 1$, which is the case if the overlap contains a few grid points, then the overlap does not improve the convergence. We will see that it is not the case in higher dimension.

Proof of the Lemma Introduce the curve $\mathcal{F} : \tau \in \mathbb{R}^+ \mapsto f(\tau) \in \mathbb{C}$. The domain $K(c)$ is $\mathcal{F}([\tau_m, \tau_M])$. The proof has four steps.

1. Study the graph of \mathcal{F} , see Figure 1.
2. Existence and uniqueness of a minmax reached at $(s_0^*(L), \delta_0^*(L))$ follows from the theoretical results above.
3. Prove that if L is small, s is large, and Ls is small, the function $\tau \mapsto R(\tau, s, L)$ has a unique stationary point $\tau_+ \sim s/L\phi$ corresponding to a maximum.
4. Prove that for small L , there is a unique $\bar{s}_0^*(L)$ such that $R(\tau_m, s, L) = R(\tau_+, s, L)$ or $R(\tau_M, s, L)$, and that it satisfies the assumptions in the previous item.
5. Prove that $\bar{s}_0^*(L)$ is a strict real minimum point of $F(\cdot, L)$.
6. Conclude by theoretical results that $\bar{s}_0^*(L) = s_0^*(L)$.

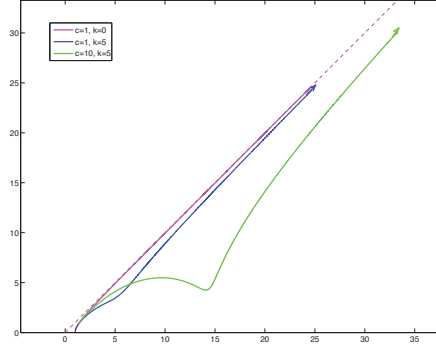


Fig. 1 Geometric representation of the function \mathcal{F} defining $K(c)$, for $c = 1, k = 0$ (magenta), $c = 1, k = 5$ (blue), $c = 10, k = 5$ (green). The direction of increasing τ is indicated by the arrow.

The real and imaginary parts of f , $x(\tau)$ and $y(\tau)$, are defined by:

$$\begin{cases} x^2 - y^2 = a_1^2 + 4\nu \frac{kc\tau^2\phi^2}{k^2 + \tau^2\phi^2}, \\ 2xy = 4\nu\tau\phi \left(1 + \frac{k^2c}{k^2 + \tau^2\phi^2}\right), \\ x \geq x_m > 0, \quad y \geq 0. \end{cases} \quad (15)$$

In the (x, y) plane, the curve \mathcal{F} lies between the real axis and the bisectrix ($y = x$). For further investigations, the derivatives of x and y are needed. To simplify the notations, introduce

$$\omega = \phi\tau, \quad g_1(s) = \frac{k^2}{s + k^2}, \quad g_2(s) = 1 - cg_1(s) + 2cg_1(s)^2,$$

and differentiate (15) to obtain the derivatives of x and y , in terms of x, y, g_1 , and g_2 as:

$$\begin{cases} x^2 - y^2 = a_1^2 + 4\nu kc(1 - g_1(\omega^2)) \\ 2xy = 4\nu\omega(1 + cg_1(\omega^2)) \end{cases}, \quad \begin{pmatrix} \partial_\tau x \\ \partial_\tau y \end{pmatrix} = \frac{2\nu\phi}{x^2 + y^2} \begin{pmatrix} \frac{2c}{k}\omega g_1^2(\omega^2)x + g_2(\omega^2)y \\ -\frac{2c}{k}\omega g_1^2(\omega^2)y + g_2(\omega^2)x \end{pmatrix}. \quad (16)$$

The zeros of $\partial_\tau x$ exist only at points τ with $g_2(\omega^2) < 0$, which happens only if $c > 8$ and $g_1(\omega^2) \in]\tilde{g}_1^1, \tilde{g}_1^2[\subset]0, 1[$, with $\tilde{g}_1^1 = \frac{c - \sqrt{c^2 - 8c}}{4c}$ and $\tilde{g}_1^2 = \frac{c + \sqrt{c^2 - 8c}}{4c}$. Accordingly $\partial_\tau y$ vanishes only at points τ with $g_2(\omega^2) > 0$, which happens if $c > 8$ and $g_1(\omega^2) \notin]\tilde{g}_1^1, \tilde{g}_1^2[$, or $c < 8$.

To solve $\partial_\tau x = 0$, it will be easier to rewrite it in terms of $g_1(\omega^2) < 0$ only. To do so, multiply the equation $\partial_\tau x = 0$ successively by x and by y , then replace $xy = 2\nu\omega(1 + cg_1)$. In the resulting equation replace $\omega^2 g_1(\omega^2) = k^2(1 - g_1(\omega^2))$,

and finally insert these values into the equation $x^2 - y^2 = a_1^2 + 4vk c(1 - g_1(\omega^2))$, to obtain that $\partial_{\tau}x(\tau) = 0$ is equivalent to

$$g_1(\omega^2) \text{ is a root of } Q \text{ in } (\tilde{g}_1^1, \tilde{g}_1^2), \text{ with} \\ Q(X) = -4c^2(c + 2b + 2)X^4 + c^2(3c + 4b + 8)X^3 - c(3c + 4b + 4)X^2 + cX - 1.$$

Computing the derivatives of Q , it is easy to see that Q has a maximum point in $(0, 1)$. Since Q has alternate coefficients, it cannot have negative zeros. Compute $Q(0) = -1$, $Q(1) < 0$. $Q(\tilde{g}_1^j) = 4c^2(\tilde{g}_1^j)^3(1 - \tilde{g}_1^j)(1 + c\tilde{g}_1^j) > 0$. This proves that Q has two roots in $(0, 1)$, outside $(\tilde{g}_1^1, \tilde{g}_1^2)$, which indeed correspond to zeros of $\partial_{\tau}y$. This implies that x is an increasing function of τ , y' vanishes for two values of τ , and the curve has the behavior depicted in Figure 1.

2. Rewrite the convergence factor R with $L = 2v\ell$ as

$$R_0(\tau, s) = \frac{(x-s)^2 + y^2}{(x+s)^2 + y^2}, \quad R(\tau, s, L) = R_0(\tau, s)e^{-2\ell x}$$

Compute for fixed s the derivative of R with respect to τ .

$$\partial_{\tau}R(\tau, p, L) = (\partial_{\tau}R_0(\tau, s) - 2\ell\partial_{\tau}xR_0(\tau, s))e^{-2\ell x} = \frac{2v\phi S(\tau, p, \ell)}{|f|^2|f+p|^4}$$

with

$$S(\tau, s, \ell, c) = (4s(x^2 - y^2 - s^2) - 2\ell|f^2 - s^2|^2) \left(\frac{2c}{k} \omega g_1^2 x + g_2 y \right) + 8sxy \left(-\frac{2c}{k} \omega g_1^2 y + g_2 x \right).$$

Suppose ℓ small, s large, and ℓs small. For $c = 0$, S is a bi-quadratic polynomial in the x variable

$$\tilde{S}(x, s, \ell) = -4\ell x^4 + 4(\ell b^2 + s)x^2 - \ell b^2(b^2 - 2s^2) + 2s(b^2 - s^2).$$

\tilde{S} has two positive roots, which behave asymptotically as $x_- \sim s$ and $x_+ \sim \sqrt{s/\ell}$, corresponding to two values of τ , $\tau_- \sim \frac{s^2}{2v\phi} \ll \tau_+ \sim \frac{s}{2v\ell\phi}$. Since R tends to 0 at infinity, τ_- corresponds to a minimum, and τ_+ to a maximum of R .

We now extend the solution to positive c . A careful computation shows that

$$\partial_c S(\tau_{\pm}, s, \ell, c) \sim 16svx_{\pm} \neq 0.$$

Therefore, by the implicit function theorem, in a neighborhood of 0, $0 \leq c \leq c_0$, the root τ_- (resp. τ_+) continues in a minimum point $\tau_-(c)$, (resp. maximum point $\tau_+(c)$) with $\tau_{\pm}(0) = \tau_{\pm}$. They have the same asymptotic behavior $\tau_+(c) \sim s/2v\ell$ (resp. $\tau_-(c) \sim s^2/2v$) independent of c , and one can iterate the argument, showing for any c the existence of a function $\tau_+(c) \sim \frac{s}{2v\ell\phi}$ (resp. $\tau_-(c) \sim \frac{s^2}{2v}$) with $S(\tau_{\pm}(c), s, \ell, c) = 0$. They remain indeed global maximal and minimal points: suppose that there exists another root τ of S , and examine its asymptotic behavior. Since $\partial_{\tau}x(\tau) > 0$, it can not be at finite distance, since then we would have

$S(\tau, p, \ell, c) \sim -4s^3x' < 0$. Suppose now that $\tau \simeq \ell^{-\theta}$ with $\theta > 0$. Then the principal part of S is:

$$-4\ell(x(\tau))^4 + 4p(x(\tau))^2 - p^3(p\ell + 2)$$

whose roots are equivalent to those of S , proving that there is no other extremal point than $\tau_{\pm}(c)$. Then

$$\sup_{\tau \in K} R(\tau, s, L) = \begin{cases} \max(R(\tau_m, s, L), R(\tau_+, s, L)) & \text{if } \tau_+ < \tau_M, \\ \max(R(\tau_m, s, L), R(\tau_M, s, L)) & \text{if } \tau_+ > \tau_M, \end{cases}$$

3 Compute now $\partial_s R(\tau, s, L) = (\partial_s R(\tau, s, 0))e^{-\ell x}$. It is easy to see that $R(\tau_m, s, L)$ is an increasing function of s , $R(\tau_+, s, L)$ a decreasing function of s , and $R(\tau_M, s, L)$ has a minimum reached for $s = |f(\tau_M)|$.

If $\lambda < \frac{3}{4}$, asymptotic considerations show that there exists a \bar{s}_0^* such that $R(\tau_m, s, L) - R(\tau_+, s, L) = 0$, and that

$$\sup_{\tau \in K} R(\tau, s, L) = \begin{cases} R(\tau_+, s, L) & \text{for } s < \bar{s}_0^*, \\ R(\tau_m, s, L) & \text{for } s > \bar{s}_0^*. \end{cases}$$

The other case is similar.

4 To prove that it is a strict local minimum, proceed as in [1] and evaluate asymptotically the sign of $\partial_p R(\tau_+, \bar{s}_0^*(L), L) \times \partial_p R(\tau_m, \bar{s}_0^*(L), L) < 0$.

2.1 Performances of different transmission conditions

In this test case in $\Omega = (0, 1) \times (0, 1)$, the diffusion parameter is $\nu = 1$, advection is $\mathbf{a} = (1 \cdot 10^{-2}, 5 \cdot 10^{-2})$, the reactivity coefficient is set to $k = 5$ with an equilibrium parameter of $c = 10$. The finite volumes method is described in [8]. The discretization parameters are $\Delta t = \Delta x = \Delta y = 2 \cdot 10^{-2}$. The domain Ω is split into $\Omega_1 = [0, 0.5 + L] \times [0, 1]$ and $\Omega_2 = [0.5, 1] \times [0, 1]$. A minimal overlap of size $L = \Delta x$ is used. A random initial guess is imposed on the interface Γ_1 . The results are plot in Figure 2. The expected behavior takes place. The best convergence behaviour is obtained with optimised Ventcel conditions with overlap which reach the error precision of 10^{-10} in only 6 iterations.

3 Newton-Schwarz waveform relaxation for the nonlinear system

The Schwarz waveform relaxation algorithm was used for the semilinear heat equation $\partial_t u - c^2(x)\partial_{xx}u + f(u) = 0$ in [5]. Under the condition that $f'(x) \leq a$, the same convergence behavior as in the linear case was exhibited and analyzed. Optimized Schwarz waveform relaxation algorithm, with nonlinear transmission con-

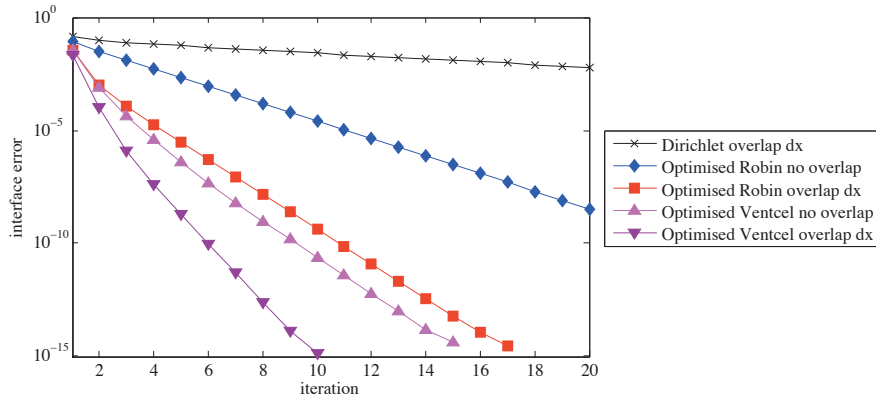


Fig. 2 Iterations versus error of the domain decomposition iterates

ditions were first introduced in [11], for the semilinear wave equation. In [3], the semilinear advection-diffusion reaction equation in 2 dimensions was considered, $\partial_t u - \nu \Delta u + f(u) = 0$, where f is constrained only to be in $C^2(\mathbb{R})$, with $f(0) = 0$. Nonoverlapping Robin-Schwarz and Ventcell-Schwarz were proposed and analyzed. The main difficulty in this case is that each iterate in Table 1 is solution of a nonlinear problem, whose solution has to be defined properly, and has its own time of existence T_j^n . The sequence $(T_j^n)_n$ is decreasing, and it must be shown that there is a lower bound T_* for these times. Then the convergence is achieved inside $(0, T_*)$. From a numerical point of view, a nonlinear system has to be solved in each subdomain at every step, which has been implemented with \mathbf{P}_1 finite elements in space, and a linearly implicit Euler scheme in time. It turns out that the requirement of small time interval given by the existence analysis is not compelling (see also [11]). Furthermore nonlinear transmission condition where the coefficients p and q depend on the iterates through the formulas of §1 were successfully implemented.

For the nonlinear reactive transport system, with suitable assumptions on the coefficients, the same methods apply, for the existence and convergence analysis (see below). However, acceleration must be obtained. This has been done in F. Häberlein's thesis [8], where several scenarios were studied. First, writing the Schwarz iteration in an interface structuring manner, it is seen as a fixed point iteration for the interface problem, preconditioned by the domain decomposition with transmission conditions given by the \mathcal{B}_j . It will be called *Classical approach*. For steady elliptic problems, the resolution of the interface problem is accelerated by a Krylov algorithm (see [17]). In this time-dependent non-linear frame, it is treated by a Newton-Krylov algorithm (called *Nested Iteration Approach*). Each iteration requires the resolution of smaller time-dependent nonlinear systems in the subdomains. This approach has been successfully implemented and described in [9]. An interesting other approach is called *Common iteration approach*. It is a Newton-Schwarz Krylov approach (see [12]) with the Jacobian explicitly computed.

$$U^{k+1} = U^k + h, \quad \partial_t h - \nu \Delta h + f'(U^k)h = -(\partial_t U^k - \nu \Delta U^k + f(U^k)).$$

The linear problem above is solved by an optimized Ventcell-Schwarz domain decomposition algorithm, accelerated by Krylov. The approach requires in every iteration of the outer loop (indices in n) to set up a right hand side-vector that demands to solve two linear problems in the subdomains. Moreover, in the matrix-vector multiplication inside the Krylov-method, only linear problems in the subdomains are evaluated. No nested nonlinear iterative method is needed. For this reason and in contrast to the approach above, this approach was called 'Common Iteration Approach' (CIA) due to the common iterative approach of the nonlinear character of the monodomain problem. The name "Newton-Schwarz-Krylov" can be used in order to explain the order of application of the different numerical tools: The global problem is first attacked by a Newton-type method. At every iteration, the resulting linear problem is decomposed by a Schwarz-type algorithm where the problem is reduced to the interface variables. The resulting linear system is then solved by a Krylov-type method.

The next simulation shows nonoverlapping Robin-Schwarz simulations in domain $\Omega = [0, 1] \times [0, 1] \subset \mathbb{R}^2$ with the subdomains $\Omega_1 = [0, 0.5] \times [0, 1]$ and $\Omega_2 = [0.5, 1] \times [0, 1]$. The considered time window is $t \in [0, 1]$. Physical parameters are $\phi = 1$, $\nu = 1.5$, $\mathbf{a} = (5 \cdot 10^{-2}, 1 \cdot 10^{-3})$. The nonlinear coupling term is defined by $R(u, v) = k(v - \Psi(u))$ where

$$\Psi(u) = \frac{Q_S K_L u}{(1 + K_L u - K_S u)(1 - K_S u)}$$

is the BET isotherm law with $k = 100$, $Q_S = 2$, $K_S = 0.7$ and $K_L = 100$ (cf. figure 3, left). BET theory is a rule for the physical adsorption of gas molecules on a solid surface and serves as the basis for an important analysis technique for the measurement of the specific surface area of a material. One observes the quadratic convergence

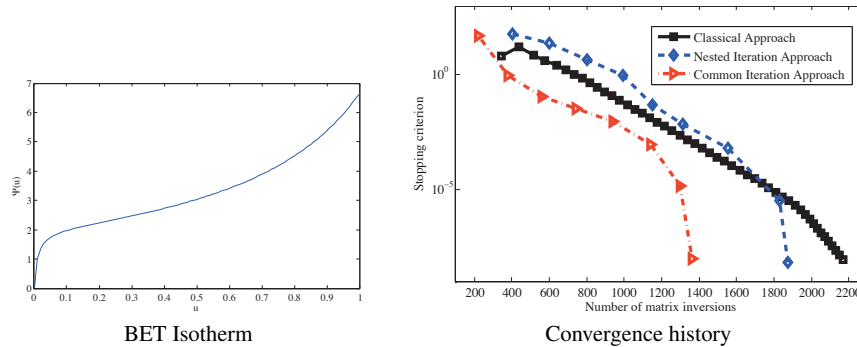


Fig. 3 Nonlinear simulation with 200 points per space dimension

of the new approaches since they are Newton-based, the quadratic convergence is

observed late in the history since the initial guess (randomly chosen) is far from the exact solution. The classical approach shows only a superlinear convergence, also in this case, the superlinear character appears late in the convergence history.

The proof of convergence for the fixed point algorithms goes as follows:

1. Define the iterates in the relevant Sobolev spaces, which is a little more difficult in the overlapping case due to the use of trace theorems (see [6] and [2]).
2. Prove the existence of a existence time independent of the iteration number.
3. Prove the convergence by energy estimates.

The first two items, and the third one in the nonoverlapping case can be obtained as in [3]. In the overlapping case, a new method has been introduced in [18]. The idea is to obtain a decay of a weighted error in time (weight $e^{-\alpha t}$) and in the direction normal to the interface (weight $\varphi(x_1)$ to be chosen to decay the energy). The strategy applies here. However, there is no proof of quadratic convergence of the Newton-based algorithms yet, even though clear evidence is given in Figure 3.

References

1. Bennequin, D., Gander, M.J., Gouarin, L., Halpern, L.: Optimized Schwarz waveform relaxation for advection reaction diffusion equations in two dimensions (2013). In preparation
2. Bennequin, D., Gander, M.J., Halpern, L.: A homographic best approximation problem with application to optimized Schwarz waveform relaxation. *Math. of Comp.* **78**(265), 185–232 (2009)
3. Caetano, F., Halpern, L., Gander, M., Szeftel, J.: Schwarz waveform relaxation algorithms for semilinear reaction-diffusion. *Networks and heterogeneous media* **5**(3), 487–505 (2010)
4. Cissé, I.: Décomposition de domaines pour des structures hétérogènes. Ph.D. thesis, Université Paris 13 (2011)
5. Gander, M.J.: A waveform relaxation algorithm with overlapping splitting for reaction diffusion equations. *Numer. Linear Alg. Appl* **6**, 125–145 (1998)
6. Gander, M.J., Halpern, L.: Optimized Schwarz waveform relaxation methods for advection reaction diffusion problems. *SIAM J. Numer. Anal.* **45**(2), 666–697 (2007)
7. Gander, M.J., Stuart, A.M.: Space time continuous analysis of waveform relaxation for the heat equation. *SIAM J. Sci. Comput.* **19**, 2014–2031 (1998)
8. Häberlein, F.: Time-space domain decomposition methods for reactive transport applied to CO_2 geological storage. PhD Thesis, University Paris 13 (2011)
9. Häberlein, F., Halpern, L., Michel, A.: Schwarz waveform relaxation and Krylov accelerators for nonlinear reactive transport. In: R.E. Bank, M.J. Holst, O.B. Widlund, J. Xu (eds.) *Domain Decomposition Methods in Science and Engineering XX*, pp. 409–416. Springer (2013)
10. Halpern, L.: Optimized Schwarz waveform relaxation: roots, blossoms and fruits. In: *Domain Decomposition Methods in Science and Engineering XVIII, Lect. Notes Comput. Sci. Eng.*, vol. 70, pp. 225–232. Springer (2009)
11. Halpern, L., Japhet, C., Szeftel, J.: Optimized Schwarz waveform relaxation and discontinuous Galerkin time stepping for heterogeneous problems. *SIAM J. on Numer. Anal.* **50**(5), 2588–2611 (2012)
12. Knoll, D., Keyes, D.: Jacobian-free newton–krylov methods: a survey of approaches and applications. *J. of Comp. Phys.* **193**, 357–397 (2004)
13. Lelarasmee, E., Ruehli, A.E., Sangiovanni-Vincentelli, A.L.: The waveform relaxation method for time-domain analysis of large scale integrated circuits. *IEEE Trans. on CAD of IC and Syst.* **1**, 131–145 (1982)

14. Lions, P.L.: On the Schwarz alternating method. I. In: R. Glowinski, G.H. Golub, G.A. Meurant, J. Périaux (eds.) First International Symposium on Domain Decomposition Methods for Partial Differential Equations, pp. 1–42. SIAM, Philadelphia, PA (1988)
15. Lions, P.L.: On the Schwarz alternating method. III: a variant for nonoverlapping subdomains. In: T.F. Chan, R. Glowinski, J. Périaux, O. Widlund (eds.) Third International Symposium on Domain Decomposition Methods for Partial Differential Equations, held in Houston, Texas, March 20–22, 1989. SIAM, Philadelphia, PA (1990)
16. Schwarz, H.A.: Über einen Grenzübergang durch alternierendes Verfahren. Vierteljahrsschrift der Naturforschenden Gesellschaft in Zürich **15**, 272–286 (1870)
17. Toselli, A., Widlund, O.: Domain Decomposition Methods - Algorithms and Theory, *Springer Series in Computational Mathematics*, vol. 34. Springer (2005)
18. Tran, M.B.: Overlapping domain decomposition: Convergence proofs. In: R.E. Bank, M.J. Holst, O.B. Widlund, J. Xu (eds.) Domain Decomposition Methods in Science and Engineering XX, *Lect. Notes Comput. Sci. Eng.*, vol. 91, pp. 519–526. Springer (2013)

References

1. Bennequin, D., Gander, M.J., Gouarin, L., Halpern, L.: Optimized Schwarz waveform relaxation for advection reaction diffusion equations in two dimensions (2013). In preparation
2. Bennequin, D., Gander, M.J., Halpern, L.: A homographic best approximation problem with application to optimized Schwarz waveform relaxation. *Math. of Comp.* **78**(265), 185–232 (2009)
3. Caetano, F., Halpern, L., Gander, M., Szeftel, J.: Schwarz waveform relaxation algorithms for semilinear reaction-diffusion. *Networks and heterogeneous media* **5**(3), 487–505 (2010)
4. Cissé, I.: Décomposition de domaines pour des structures hétérogènes. Ph.D. thesis, Université Paris 13 (2011)
5. Gander, M.J.: A waveform relaxation algorithm with overlapping splitting for reaction diffusion equations. *Numer. Linear Alg. Appl* **6**, 125–145 (1998)
6. Gander, M.J., Halpern, L.: Optimized Schwarz waveform relaxation methods for advection reaction diffusion problems. *SIAM J. Numer. Anal.* **45**(2), 666–697 (2007)
7. Gander, M.J., Stuart, A.M.: Space time continuous analysis of waveform relaxation for the heat equation. *SIAM J. Sci. Comput.* **19**, 2014–2031 (1998)
8. Häberlein, F.: Time-space domain decomposition methods for reactive transport applied to CO_2 geological storage. PhD Thesis, University Paris 13 (2011)
9. Häberlein, F., Halpern, L., Michel, A.: Schwarz waveform relaxation and Krylov accelerators for nonlinear reactive transport. In: R.E. Bank, M.J. Holst, O.B. Widlund, J. Xu (eds.) Domain Decomposition Methods in Science and Engineering XX, pp. 409–416. Springer (2013)
10. Halpern, L.: Optimized Schwarz waveform relaxation: roots, blossoms and fruits. In: Domain Decomposition Methods in Science and Engineering XVIII, *Lect. Notes Comput. Sci. Eng.*, vol. 70, pp. 225–232. Springer (2009)
11. Halpern, L., Japhet, C., Szeftel, J.: Optimized Schwarz waveform relaxation and discontinuous Galerkin time stepping for heterogeneous problems. *SIAM J. on Numer. Anal.* **50**(5), 2588–2611 (2012)
12. Knoll, D., Keyes, D.: Jacobian-free newton–krylov methods: a survey of approaches and applications. *J. of Comp. Phys.* **193**, 357–397 (2004)
13. Lelarasmee, E., Ruehli, A.E., Sangiovanni-Vincentelli, A.L.: The waveform relaxation method for time-domain analysis of large scale integrated circuits. *IEEE Trans. on CAD of IC and Syst.* **1**, 131–145 (1982)
14. Lions, P.L.: On the Schwarz alternating method. I. In: R. Glowinski, G.H. Golub, G.A. Meurant, J. Périaux (eds.) First International Symposium on Domain Decomposition Methods for Partial Differential Equations, pp. 1–42. SIAM, Philadelphia, PA (1988)

15. Lions, P.L.: On the Schwarz alternating method. III: a variant for nonoverlapping subdomains. In: T.F. Chan, R. Glowinski, J. Périaux, O. Widlund (eds.) Third International Symposium on Domain Decomposition Methods for Partial Differential Equations , held in Houston, Texas, March 20-22, 1989. SIAM, Philadelphia, PA (1990)
16. Schwarz, H.A.: Über einen Grenzübergang durch alternierendes Verfahren. Vierteljahrsschrift der Naturforschenden Gesellschaft in Zürich **15**, 272–286 (1870)
17. Toselli, A., Widlund, O.: Domain Decomposition Methods - Algorithms and Theory, *Springer Series in Computational Mathematics*, vol. 34. Springer (2005)
18. Tran, M.B.: Overlapping domain decomposition: Convergence proofs. In: R.E. Bank, M.J. Holst, O.B. Widlund, J. Xu (eds.) Domain Decomposition Methods in Science and Engineering XX, *Lect. Notes Comput. Sci. Eng.*, vol. 91, pp. 519–526. Springer (2013)